

# Correlation trends in the ground state static electric dipole polarizabilities of closed-shell atoms and ions

Yashpal Singh\* and B. K. Sahoo †

*Theoretical Physics Division, Physical Research Laboratory, Navrangpura, Ahmedabad - 380009, India*

B. P. Das

*Theoretical Physics and Astrophysics Group, Indian Institute of Astrophysics, Bangalore-560034, India*

We employ the closed-shell perturbed relativistic coupled-cluster (RCC) theory developed by us earlier [Phys. Rev. A **77**, 062516 (2008)] to evaluate the ground state static electric dipole polarizabilities ( $\alpha_s$ ) of several atomic systems. In this work, we have incorporated a class of higher order many-body effects in our calculations that had not been taken into account in the above paper. We highlight their importance in improving the accuracies of  $\alpha_s$ . We also calculate the ground state  $\alpha_s$  of the inert gas atoms and several iso-electronic singly and doubly charged ions in order to make a comparative studies of the trends of the correlation effects. Furthermore, we have developed a method to construct intermediate diagrams that are required for the computations of the unperturbed singles and doubles coupled-cluster amplitudes. Our RCC results are compared with those of many-body perturbation theory at different orders to demonstrate the importance of higher order correlation effects for the accurate determination of ( $\alpha_s$ ) of the systems that we have considered.

PACS numbers: 31.15.ap, 31.15.bw, 31.15.ve, 31.15.xp

## I. INTRODUCTION

The subject of atom-light interaction has received considerable attention with the advent of sophisticated techniques to trap and cool atomic systems and measure their properties to very high precision [1]. An accurate knowledge of the electric dipole polarizabilities of the atomic states are essential in these experiments as they are required in the studies of atomic interactions in optical lattices, atomic clocks, quantum information and many other important areas of atomic and molecular physics [2–4]. This range of applications of electric dipole polarizabilities ( $\alpha$ ) puts a premium on their accurate determination in atomic systems. Precise measurements of  $\alpha$  are challenging and involve using a number of techniques like deflection of atomic beam by electric field [5], E-H balance method [6–8], atom interferometry [9, 10], cold atom velocity change [11] et cetera. In fact, the ground state  $\alpha$  of many atomic systems are not yet measured very precisely owing to difficulties in eliminating some of the larger systematics. Therefore, accurate theoretical studies of electric dipole polarizabilities in atomic systems are of particular interest.

Dalgarno and his collaborators initiated work on the polarizabilities of many-electron atoms more than five decades ago [12, 13]. Currently one of the most advanced approaches to this property is based on the linear response coupled cluster theory [14–21]. We had formulated a relativistic coupled-cluster (RCC) method to calculate polarizabilities in which the electric dipole

operator was effectively treated as a perturbation [22]. The first order perturbed RCC wave function in this case was obtained by solving an inhomogeneous equation, thereby circumventing the sum-over-states approach [22–24]. This method has been used to compute the polarizabilities of the ground states for a number of atomic systems [25–28]. In this work, we apply our method to some systems that we had studied earlier in addition to many new candidates for acquiring insights into the behavior of electron correlation in the calculations of the static electric dipole polarizabilities of these systems. We have included higher order non-linear RCC terms through special computational techniques, thereby improving our previous results. We present our Dirac-Fock (DF), third order many-body perturbation theory (MBPT(3)) and RCC results to show the quantitative changes in correlation effects in the passage from finite order MBPT to RCC and we offer explanations for this behavior.

The rest of the paper is organized as follows: In the next section, we present briefly the theory of static electric dipole polarizability and the basic working equations for its evaluation in the framework of the method that we have developed. Then, we describe the procedure for obtaining the atomic wave function and the electric dipole polarizability using the RCC method. This is followed by discussions of our results which are compared with the other calculations and measurements. We use atomic units (au) in this paper.

---

\*Email: yashpal@prl.res.in

†Email: bijaya@prl.res.in

## II. THEORY

### A. Theory of static dipole polarizability

The second order change in the energy of an atomic state  $|\Psi_n^{(0)}\rangle$  when placed in an external weak electric field  $\mathbf{E} = \mathcal{E}\hat{r}$  is given by

$$\delta E = -\frac{1}{2}\alpha\mathcal{E}^2 \quad (1)$$

where  $\alpha$  is known as the static electric dipole polarizability of the state which can be mathematically expressed using the second order perturbation theory as

$$\alpha = -\frac{2}{\langle\Psi_n^{(0)}|\Psi_n^{(0)}\rangle} \sum_I \frac{|\langle\Psi_n^{(0)}|D|\Psi_I^{(0)}\rangle|^2}{E_n^{(0)} - E_I^{(0)}}, \quad (2)$$

where the summation over  $I$  represents the inclusion of all possible intermediate states  $|\Psi_I^{(0)}\rangle$  and  $E_I^{(0)}$ s are the energies of the respective states denoted by the index in the subscripts. It is possible to determine  $\alpha$  by calculating the second order derivative of the energy shift given by Eq. (1) with respect to the electric field strength  $\mathcal{E}$ . A straightforward approach would be to sum over the intermediate states explicitly in Eq. (2). However, this is not very practical from a numerical point of view. In the method that we used earlier, polarizabilities can be determined without summing over intermediate states. In that approach, we express Eq. (2) as

$$\alpha = -2 \frac{\langle\Psi_n^{(0)}|D|\Psi_n^{(1)}\rangle}{\langle\Psi_n^{(0)}|\Psi_n^{(0)}\rangle}, \quad (3)$$

where  $|\Psi_n^{(1)}\rangle$  is a modified wave function similar to the first order perturbed wave function of  $|\Psi_n^{(0)}\rangle$  which is given by

$$|\Psi_n^{(1)}\rangle = \sum_I |\Psi_I^{(0)}\rangle \frac{|\langle\Psi_I^{(0)}|D|\Psi_n^{(0)}\rangle|}{E_n^{(0)} - E_I^{(0)}}. \quad (4)$$

It is clear that  $|\Psi_n^{(1)}\rangle$  is obtained by perturbing  $|\Psi_n^{(0)}\rangle$  by the vector operator  $D$ . Therefore,  $|\Psi_n^{(1)}\rangle$  can be obtained by solving the inhomogeneous equation

$$(H - E_n)|\Psi_n^{(1)}\rangle = -D|\Psi_n^{(0)}\rangle. \quad (5)$$

This procedure is similar in spirit to the approach given in [12] in the sense that our first order perturbed wave function is obtained from an inhomogeneous equation rather than by summing over intermediate states. To be specific, in the present work  $|\Psi_n^{(1)}\rangle$  is the first order correction to the atomic wave function with the electric dipole operator as the perturbation. Now expressing the total wave function as  $|\Psi_n\rangle = |\Psi_n^{(0)}\rangle + \lambda|\Psi_n^{(1)}\rangle$  and owing to the fact that  $D$  is an odd hermitian operator, we have

$$\alpha = \frac{\langle\Psi_n|D|\Psi_n\rangle}{\langle\Psi_n|\Psi_n\rangle}, \quad (6)$$

from keeping terms up to linear in the arbitrary parameter  $\lambda$ .

### B. Generalized Bloch equation for two external perturbations

The generalized Bloch equation for the model Hamiltonian  $H_0$  and the interaction term  $V$  is given by [29]

$$[\Omega, H_0]P = QV\Omega P - \chi PV\Omega P, \quad (7)$$

where  $P$  and  $Q$  are the projection operators corresponding to the model and orthogonal spaces respectively and  $\Omega = 1 + \chi$  is the wave operator that generates the atomic state function from the reference state  $|\Phi_n\rangle$  of a Hamiltonian say  $H_0$ ; i.e.  $|\Psi_n\rangle = \Omega|\Phi_n\rangle$ . By expanding the wave operator order by order, we obtain the following working equation

$$[\Omega^{(k)}, H_0]P = QV\Omega^{(k-1)}P - \sum_{m=1}^{k-1} \Omega^{(k-m)}PV\Omega^{(m-1)}P, \quad (8)$$

where  $\Omega^{(0)} = 1$  and the superscript  $k$  represents orders of  $V$  present in the evaluation of  $\Omega^{(k)}$ . When there are two sources of perturbation, we can still express  $|\Psi_n\rangle = \Omega|\Phi_n\rangle$  with the new perturbation potential  $V = V_1 + V_2$ . In this case, the  $k^{th}$  order  $\Omega^{(k)}$  is redefined by  $\Omega^{(\beta, \delta)}$  such that  $k = \beta + \delta$  for the  $\beta$  orders of  $V_1$  and  $\delta$  orders of  $V_2$ . In this case, the corresponding Bloch equation is expressed by [30]

$$\begin{aligned} [\Omega^{(\beta, \delta)}, H_0]P &= QV_1\Omega^{(\beta-1, \delta)}P + QV_2\Omega^{(\beta, \delta-1)}P - \\ &\sum_{m=1}^{\beta-1} \sum_{l=1}^{\delta-1} (\Omega^{(\beta-m, \delta-l)}PV_1\Omega^{(m-1, l)}P - \\ &\Omega^{(\beta-m, \delta-l)}PV_2\Omega^{(m, l-1)}P), \end{aligned} \quad (9)$$

with  $\Omega^{(0,0)} = 1$ ,  $\Omega^{(1,0)} = V_1$  and  $\Omega^{(0,1)} = V_2$ . In this procedure, the atomic state function up to  $k^{th}$  order is given by

$$|\Psi_n^{(k)}\rangle = [\Omega^{(k,0)} + \sum_{\delta=1}^{k-1} \lambda^\delta \Omega^{(k-\delta, \delta)}]|\Phi_n\rangle, \quad (10)$$

where we have introduced a parameter  $\lambda$  without any loss of generality to keep track of the order of  $V_2$  and it can be later set to one in the final consideration.

Using the above prescription in Eqs. (5) and (3), it yields

$$|\Psi_n^{(k,0)}\rangle = \Omega^{(k,0)}|\Phi_n\rangle \quad (11)$$

and its first order correction due to  $V_2$  is given by

$$|\Psi_n^{(k,1)}\rangle = \Omega^{(k,1)}|\Phi_n\rangle. \quad (12)$$

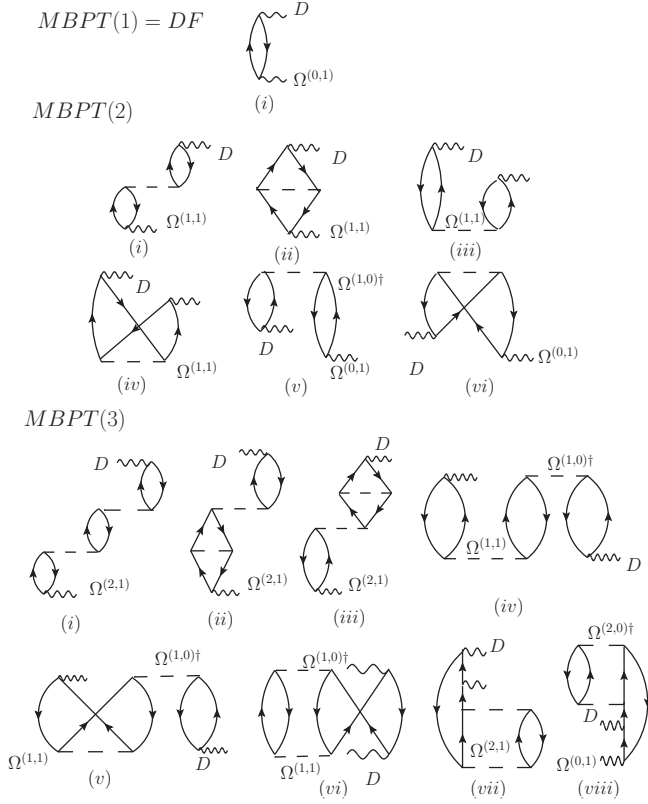


FIG. 1: Few important contributing diagrams of the MBPT(3) method. The lowest order contribution is given as the DF result.

In our present work, the residual interaction  $V_{es}$  is treated as the first perturbation ( $V_1 = V_{es}$ ) to include the electron correlation effects in a many-body perturbation treatment and we set  $V_2 = D$  and  $\delta = 1$  for calculating  $\alpha$ . In this approach, the lowest and  $k^{th}$  order results for  $\alpha$  is given by

$$\alpha = 2\langle\Psi_n|D\Omega^{(0,1)}|\Psi_n\rangle. \quad (13)$$

and

$$\alpha = 2\frac{\sum_{\beta=0}^{k-1}\langle\Psi_n|\Omega^{(k-\beta-1,0)\dagger}D\Omega^{(\beta,1)}|\Psi_n\rangle}{\sum_{\beta=0}^{k-1}\langle\Psi_n|\Omega^{(k-\beta-1,0)\dagger}\Omega^{(\beta,0)}|\Psi_n\rangle}, \quad (14)$$

respectively.

### III. METHOD OF CALCULATIONS

The Dirac-Coulomb (DC) atomic Hamiltonian which is used in our calculation is given by

$$H^{DC} = \sum_i \left[ c\alpha_i \cdot \mathbf{p}_i + (\beta_i - 1)c^2 + V_{nuc}(r_i) + \sum_{j>i} \frac{1}{r_{ij}} \right] \quad (15)$$

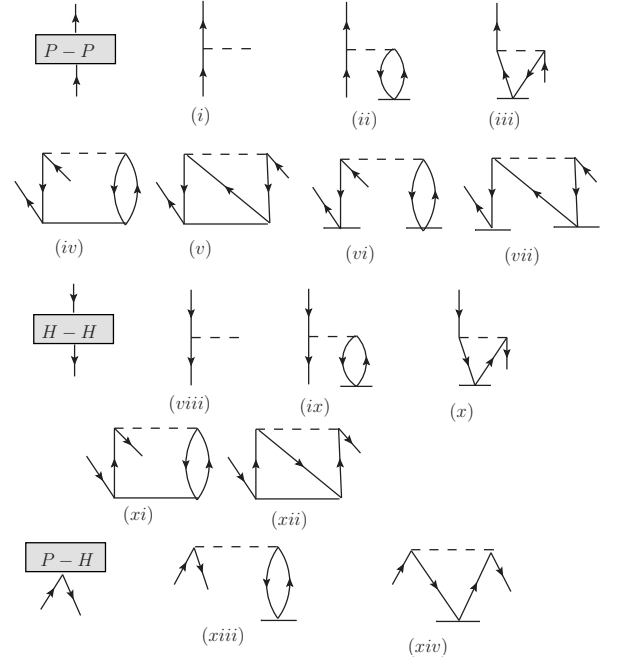


FIG. 2: Effective one-body intermediate diagrams for the evaluation of CCSD amplitudes.

The single particle energies are scaled with respect to the rest mass energy of the electron, the nuclear potential is evaluated considering a Fermi nuclear charge distribution and the electron-electron interaction due to one photon exchange is restricted to Coulomb interactions only.

The DF approximation ( $H_0 = H_{DF}$ ) yields the mean-field wave function  $|\Phi_0\rangle$  for the ground state which we consider as the reference state  $|\Phi_n\rangle$  for the construction of exact ground state wave function  $|\Psi_n\rangle = |\Psi_0\rangle$ .

#### A. MBPT(3) method

The importance of various correlation terms in the determination of  $\alpha$  can be better understood from an explicit analysis of lower order perturbation calculations where the contributions from the individual term can be found explicitly. For this purpose, we have considered up to  $\beta = 2$  and  $\delta = 1$  (MBPT(3) method) to calculate  $\alpha$ .

Therefore, the expression for  $\alpha$  of the ground state in the MBPT(3) method is given by

$$\begin{aligned} \alpha &= \frac{2}{\mathcal{N}} \langle \Phi_0 | [\Omega^{(0,0)} + \Omega^{(1,0)} + \Omega^{(2,0)}]^\dagger D \\ &\quad \times [\Omega^{(0,1)} + \Omega^{(1,1)} + \Omega^{(2,1)}] | \Phi_0 \rangle \\ &= \frac{2}{\mathcal{N}} \langle \Phi_0 | D\Omega^{(0,1)} + D\Omega^{(1,1)} + D\Omega^{(2,1)} + \Omega^{(1,0)\dagger} D\Omega^{(0,1)} \\ &\quad + \Omega^{(1,0)\dagger} D\Omega^{(1,1)} + \Omega^{(2,0)\dagger} D\Omega^{(0,1)} | \Phi_0 \rangle, \end{aligned} \quad (16)$$

with  $\mathcal{N} = \langle \Phi_0 | 1 + \Omega^{(1,0)} + \Omega^{(2,0)} + \Omega^{(1,0)\dagger} + \Omega^{(2,0)\dagger} + \Omega^{(1,0)\dagger} \Omega^{(0,1)} | \Phi_0 \rangle$ .

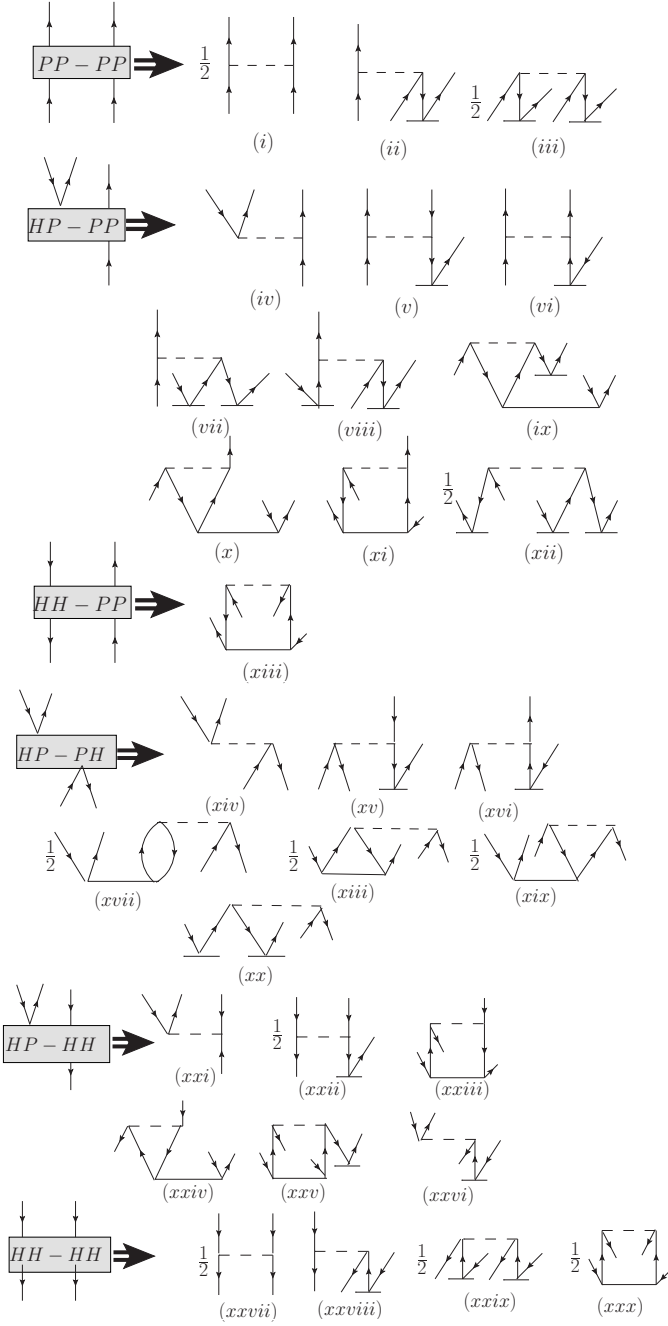


FIG. 3: Effective two-body intermediate diagrams for the evaluation of CCSD amplitudes.

The above wave operators are obtained using the fol-

lowing Bloch equations

$$\begin{aligned}
 [\Omega^{(1,0)}, H_0]P &= QV_{es}P \\
 [\Omega^{(2,0)}, H_0]P &= QV_{es}\Omega^{(1,0)}P - \Omega^{(1,0)}PV_{es}P \\
 &\text{and} \\
 [\Omega^{(0,1)}, H_0]P &= QDP \\
 [\Omega^{(1,1)}, H_0]P &= QV_{es}\Omega^{(0,1)}P + QD\Omega^{(1,0)}P \\
 [\Omega^{(2,1)}, H_0]P &= QV_{es}\Omega^{(1,1)}P + QD\Omega^{(2,0)}P - \\
 &\quad \Omega^{(1,0)}PV_{es}\Omega^{(0,1)}P - \Omega^{(1,0)}PD\Omega^{(1,0)}P.
 \end{aligned}$$

Important lower order diagrams that contribute at the MBPT(3) level are shown in Fig. 1.

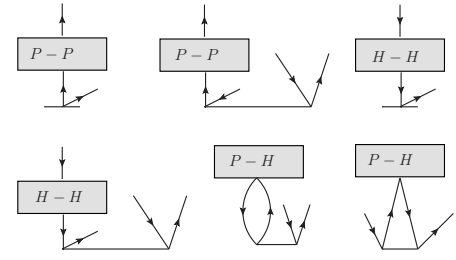


FIG. 4: Final CCSD amplitudes determining diagrams after contracting effective one-body intermediate diagrams with the  $T^{(0)}$  operators.

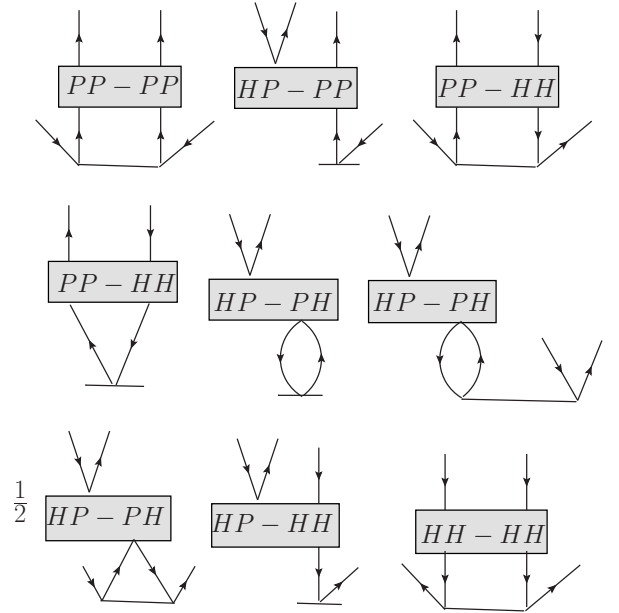


FIG. 5: Final CCSD amplitudes determining diagrams after contracting effective two-body intermediate diagrams with the  $T^{(0)}$  operators.

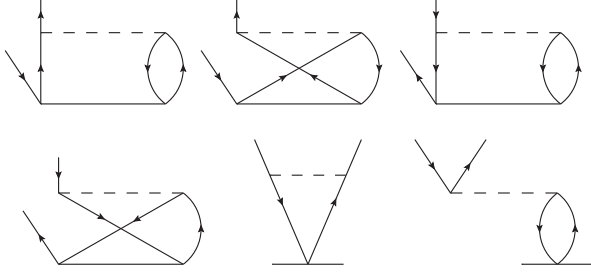


FIG. 6: Direct contributing diagrams to the singles of the CCSD method.

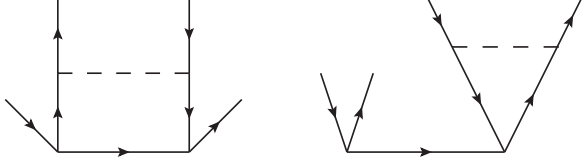


FIG. 7: Direct contributing diagrams to the doubles of the CCSD method.

### B. RCC theory: CCSD method

In the RCC theory, the ground state of a closed-shell atom is expressed as

$$\begin{aligned} |\Psi_0\rangle &= \Omega|\Phi_0\rangle \\ &= e^T|\Phi_0\rangle, \end{aligned} \quad (17)$$

where the operator  $T$  corresponds to the excitations from the reference state  $|\Phi_0\rangle$ .

Following Eq. (6), we have

$$\begin{aligned} \alpha &= \frac{\langle\Phi_0|\Omega^\dagger D\Omega|\Phi_0\rangle}{\langle\Phi_0|\Omega^\dagger\Omega|\Phi_0\rangle} \\ &= \frac{\langle\Phi_0|e^{T^\dagger} D e^T|\Phi_0\rangle}{\langle\Phi_0|e^{T^\dagger} e^T|\Phi_0\rangle}. \end{aligned} \quad (18)$$

By definition, the  $T$  operators are in normal order form with respect to the reference state  $|\Phi_0\rangle$ . Therefore, the above expression yields [31]

$$\begin{aligned} \alpha &= \frac{\langle\Phi_0|e^{T^\dagger} D_N e^T|\Phi_0\rangle_{con} \langle\Phi_0|e^{T^\dagger} e^T|\Phi_0\rangle}{\langle\Phi_0|e^{T^\dagger} e^T|\Phi_0\rangle} \\ &= \langle\Phi_0|e^{T^\dagger} D_N e^T|\Phi_0\rangle_{con}, \end{aligned} \quad (19)$$

this is a favorable denouement for the calculation of properties of the ground state of closed-shell atomic systems using the RCC theory. The subscript  $N$  represents the normal order form of  $D$  and *con* refers to survival of only the connected diagrams.

In the above RCC expression, the operator  $T$  includes contributions from both  $V_{es}$  and  $D$ . Taking this into consideration, we split  $T$  into

$$T = T^{(0)} + \lambda T^{(1)} \quad (20)$$

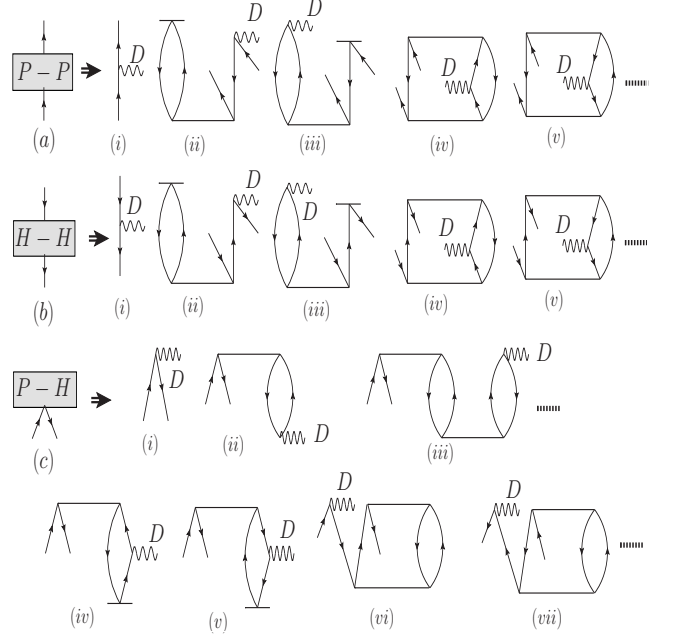


FIG. 8: Few effective one-body diagrams from  $e^{T^\dagger(0)} D_N e^{T(0)}$  that are connected further with  $T^{(1)}$  operator in the final evaluation of the polarizabilities.

where  $T^{(0)}$  corresponds to correlation effects due to  $V_{es}$  and  $T^{(1)}$  takes into account the opposite parity excitations in the wave function due to  $D$ . Substituting Eq. (20) in Eq. (17), we get

$$|\Psi_0^{(0)}\rangle = e^{T^{(0)}}|\Phi_0\rangle \quad (21)$$

and

$$|\Psi_0^{(1)}\rangle = e^{T^{(0)}} T^{(1)}|\Phi_0\rangle. \quad (22)$$

In the present work, we have considered all possible singly and doubly excited configurations (known as the CCSD method) by defining

$$T^{(0)} = T_1^{(0)} + T_2^{(0)} \quad (23)$$

and

$$T^{(1)} = T_1^{(1)} + T_2^{(1)}. \quad (24)$$

The  $T^{(0)}$  amplitudes are obtained by solving the following equation

$$\langle\Phi_0^\tau|\overline{H_N^{DC}}|\Phi_0\rangle = 0, \quad (25)$$

where  $\tau = 1, 2$  stands for either singly or doubly excited configurations from  $|\Phi_0\rangle$ , subscript  $N$  represents the normal ordered form of the DC Hamiltonian and the dressed Hamiltonian  $\overline{H_N^{DC}} = e^{-T^{(0)}} H_N^{(DC)} e^{T^{(0)}}$  which is equal to  $(H_N^{(DC)} e^{T^{(0)}})_{con}$  [32]. To solve the above equation, we adopt the Jacobi iterative procedure and the non-linear

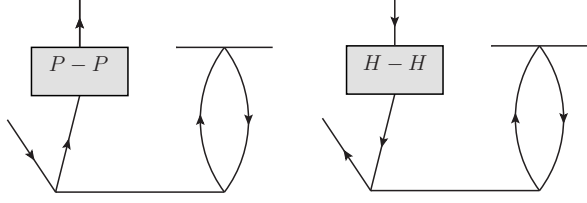


FIG. 9: Examples of further dressed-up effective H-P type diagrams from the effective P-P and H-H type one-body diagrams.

terms from  $(H_N^{(DC)} e^{T^{(0)}})_{con}$  are accounted through the intermediate diagrams. A standard procedure for defining intermediate diagrams are described in [33, 34]. However, we follow a different strategy here. The idea behind this is to avoid the repetition of defining different variables to store the intermediate diagrams. In our approach, we define some distinct types of intermediate diagrams by classifying them into effective one-body and two-body diagrams as given in Figs. 2 and 3, respectively. They are further combined with suitable  $T^{(0)}$  operators for constructing the final diagrams that contribute to the computations of the  $T_1^{(0)}$  and  $T_2^{(0)}$  amplitudes as shown in Figs. 4 and 5. The diagrams which involve fewer internal lines but are problematic for generating repetitive diagrams when included in the above effective one-body and two-body intermediate diagrams are computed directly. Examples of such diagrams for the evaluation of the  $T_1^{(0)}$  and  $T_2^{(0)}$  amplitudes are shown in Figs. 6 and 7, respectively. To avoid the double counting of topologically equivalent diagrams arising from the above effective intermediate diagrams and from symmetry considerations, we multiply by a factor of 1/2 wherever necessary as mentioned in Figs 3 and 5.

After obtaining  $T^{(0)}$  amplitudes, we solve the following equation to determine the  $T^{(1)}$  amplitudes

$$\langle \Phi_0 | \overline{H_N^{DC}} T^{(1)} | \Phi_0 \rangle = -\langle \Phi_0 | \overline{H_{int}} | \Phi_0 \rangle. \quad (26)$$

We now make use of the locations of the previously defined intermediate variables to store all possible effective one-body and two-body diagrams of  $\overline{H_N^{DC}}$ . In this case, no additional multiplicative factors are needed owing to the fact that finally these diagrams are contracted with  $T^{(1)}$  amplitudes. Also, all the contributing terms from  $T^{(0)}$  are included at this stage. Contributions from  $\overline{H_{int}} = (H_{int} e^{T^{(0)}})_{con}$  are computed directly.

With the knowledge of  $T^{(0)}$  and  $T^{(1)}$  amplitudes, we evaluate  $\alpha$  using the relation

$$\begin{aligned} \alpha &= \langle \Phi_0 | e^{T^\dagger} D_N e^T | \Phi_0 \rangle_{con} \\ &= \langle \Phi_0 | T^{\dagger(1)} \overbrace{D_N^{(0)}} + \overbrace{D_N^{(0)}} T^{(1)} | \Phi_0 \rangle_{con} \\ &= 2 \langle \Phi_0 | \overbrace{D_N^{(0)}} (T_1^{(1)} + T_2^{(1)}) | \Phi_0 \rangle_{con} \end{aligned} \quad (27)$$

where  $\overbrace{D_N^{(0)}} = e^{T^{\dagger(0)}} D_N e^{T^{(0)}}$  is a non-truncating series.

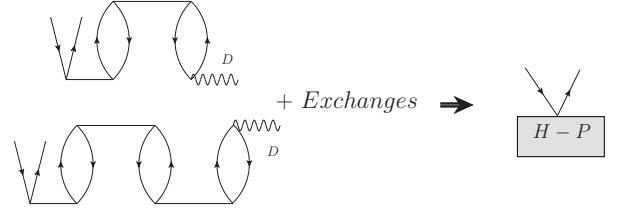


FIG. 10: Additional effective diagrams which are stored separately and contracted finally with the  $T^{(0)}T^{(1)}$  for accounting higher order core-polarization correlation effects.

We compute this by dividing it into connected effective one-body and two-body terms using the generalized Wick's theorem [29] before contracting them with  $T^{(1)}$ . In the CCSD approximation that we have considered here, we need only the fully contracted terms from  $\overbrace{D_N^{(0)}} (T_1^{(1)} + T_2^{(1)})$ . Therefore only the effective one-, two- and three-body terms will survive from  $\overbrace{D_N^{(0)}}$ . Effective one-body diagrams arising from the non-truncating series  $\overbrace{D_N^{(0)}}$  which contribute significantly are further binned into the hole-hole (H-H), particle-particle (P-P), hole-particle (H-P) and particle-hole (P-H) type diagrams as shown in Fig. 8 (H-P diagrams are not shown as they are complex conjugate (cc) terms of P-H type of diagrams) considering up to minimum fifth order in the residual Coulomb interaction. It can be noticed from Fig. 8(c) of the P-H and H-P type diagrams that they contain diagrams (e.g.  $i, ii, iii$  etc.) resembling the random phase approximation (RPA) along with some of the non-RPA diagrams (e.g.  $iv, v, vi$  etc.) which account for the core-polarization effects to all orders. We found, as will be demonstrated in the next section, they are the leading contributors. Therefore, we replace the corresponding  $D$  operator from the P-H and H-P effective diagrams by the P-P and H-H diagrams as shown in Fig. 9 to dress-up the effective H-P/P-H operators for evaluating these contributions more rigorously. These effective diagrams are then further combined with the  $T^{(1)}$  and  $T^{(0)}T^{(1)}$  operators to obtain the final contributions. The important diagrams that make significant contributions from the effective two-body and three-body terms of  $\overbrace{D_N^{(0)}}$  are computed directly after contracting them with the  $T^{(1)}$  operators.

We also store the effective H-P/P-H type one-body diagrams from  $\overbrace{D_N^{(0)}}$  having more than two orders of residual Coulomb interaction, as shown in Fig. 10 separately and contract them with another set of  $T^{(0)}T^{(1)}$  terms in the final calculations to include the contributions of core-polarization effects, higher in order than those described above. We found that these contributions are crucial for improving the final results for the alkaline earth-metal atoms that were neglected in our previous calculations

TABLE I: Ground state static dipole polarizability  $\alpha$  of various closed shell atoms and ions. In the parentheses of our results, we have given the estimated uncertainties from the calculations. The square brackets refers to the references of other works.

Systems	This Work	Others	Experiments
He	1.360(20)	1.322 [35], 1.383763 [36]	1.383223(67) [37, 38], 1.3838 [39]
Ne	2.652(15)	1.38376079(23) [40], 1.382(1) [22] 2.38 [35], 2.6648 [36], 2.697 [43]	1.384 [41], 1.383759(13) [42] 2.670(3) [44], 2.66110(3) [45]
Ar	11.089(4)	2.665 [46], 2.668(6) [47] 2.6695 [25] 10.77 [35], 11.084 [36], 11.22 [43] 11.085(6) [48] 11.213 [26]	2.6680 [39], 2.663 [41] 11.081(5) [44], 11.091 [39] 11.080 [41], 11.083(2) [49]
Kr	16.93(5)	16.47 [35], 16.80 [50], 16.736 [26]	16.766(8) [44], 16.740 [39], 16.740 [41]
Be	37.86(17)	37.755 [51], 37.73(5) [52], 37.807 [53], 37.29 [54], 37.69 [55], 37.76 [56], 37.80(47) [22]	
Mg	72.54(50)	71.7 [57], 70.90 [58], 70.74 [54], 71.35 [55], 71.33 [56], 74.9(2.7) [59], 73.41(2.32) [22]	
Ca	157.03(80)	157 [57], 171.7 [60], 156.0 [54] 159.4 [55], 158.00 [61], 152 [62] 159.0 [56], 157.1(1.3) [56], 154.58(5.42) [22]	169(17) [7]
Sr	186.98(85)	201.2 [55], 198.85 [61], 190 [62], 202.0 [56], 197.2(2) [56], 199.71(7.28) [22]	186(15) [8]
Li <sup>+</sup>	0.1913(5)	0.192486 [63, 64], 0.1894 [35]	0.1883(20) [65]
Na <sup>+</sup>	0.9984(7)	0.9947 [54], 0.9457 [35] 1.00(4) [72], 1.025 [27]	0.978(10) [66], 1.0015(15) [67] 0.9980(33) [68]
K <sup>+</sup>	5.522(7)	5.354 [54], 5.457 [35] 5.52(4) [72], 5.735 [27]	5.47(5) [66]
Rb <sup>+</sup>	9.213(15)	9.076 [35], 9.11(4) [72], 9.305[27]	9.0 [69]
Sc <sup>+</sup>	53.24(20)		
Y <sup>+</sup>	72.26(50)		
Be <sup>2+</sup>	0.0521(2)	0.05182 [35], 0.052264 [63, 64]	
Mg <sup>2+</sup>	0.4852(5)	0.4698 [69], 0.495 [28] 0.4814 [54]	0.489(5) [66] 0.486(7) [70]
Ca <sup>2+</sup>	3.295(6)	3.254 [35], 3.161 [54] 3.262 [61], 3.387 [28]	3.26(3) [66]
Sr <sup>2+</sup>	5.877(8)	5.813 [35], 5.792 [61], 5.913 [28]	

[22–24]. As they are just another set of effective one-body terms, they marginally affect the computational cost.

#### IV. RESULTS AND DISCUSSIONS

We present our polarizability results for the ground states for several atomic systems and compare them with other calculations and experimental results in Table I. We have also estimated the errors in our calculations arising from the numerical uncertainties due to the finite size of the basis, neglected contributions from the Breit interaction and QED effects due to the lowest order vacuum polarization and self-energy corrections. Moreover contributions from the Breit and QED effects are found to be small for the property under consideration here, but the size of the basis is crucial for the numerical accuracy of the calculations. We estimated contributions from the Breit and QED interactions using the MBPT(3) method by carrying out calculations with these interactions separately along with the DC Hamiltonian. Inaccuracies from the choice of basis functions are estimated in two steps using the DF method: (i) results are obtained for

different set of optimized Gaussian parameters and (ii) estimating contributions from the inactive orbitals that are not considered in the RCC calculations from the DF method. We present these estimated contributions from the individual source in Table II. Experimental results for light atomic systems are more accurate than our calculations. However, for heavy systems, the accuracies of our results are better than those of experiments and many of the previous calculations.

A variety of many-body methods have been used to determine  $\alpha$  for the systems that we have considered except for Sc<sup>+</sup> and Y<sup>+</sup>. The method we have employed in the present work had been used previously to calculate these quantities [22–24]. In those calculations,

we had truncated  $\widehat{D}_N^{(0)}$  at  $\widehat{D}_N^{(0)} = T^\dagger(0)D_NT(0)$  neglecting higher order RPA contributions coming through the  $T^\dagger(0)D_N(T(0))^2$  and  $(T^\dagger(0))^2D_NT(0)$  whose contributions are found to be significant in the neutral alkaline earth atoms, Sc<sup>+</sup> and Y<sup>+</sup>. Also the results have improved, particularly in these systems, since the dipole operators in the P-H and H-P effective diagrams described by Fig. 10 and in the construction of the effective two-body opera-

TABLE II: Contributions to the estimated uncertainties from the Breit interaction ( $\delta_B$ ), QED corrections ( $\delta_Q$ ) and finite basis size ( $\delta_F$ ) in the considered atomic systems.

System	$\delta_B$	$\delta_Q$	$\delta_F$
He	$\sim 0.0$	$\sim 0.0$	0.0200
Ne	0.0006	$\sim 0.0$	0.1499
Ar	0.0023	0.0002	0.0032
Kr	0.0148	0.0008	0.0478
Be	0.0027	-0.0001	0.1699
Mg	0.1460	-0.0008	0.4782
Ca	-0.1609	-0.0041	0.7836
Sr	-0.1767	-0.0201	0.8312
Li <sup>+</sup>	$\sim 0.0$	$\sim 0.0$	0.0005
Na <sup>+</sup>	0.0003	$\sim 0.0$	0.0004
K <sup>+</sup>	0.0004	0.0001	0.0070
Rb <sup>+</sup>	0.00960	0.0002	0.0115
Sc <sup>+</sup>	-0.0453	-0.0533	0.1874
Y <sup>+</sup>	-0.0631	-0.0089	0.4959
Be <sup>2+</sup>	$\sim 0.0$	$\sim 0.0$	0.0002
Mg <sup>2+</sup>	0.0001	$\sim 0.0$	0.0004
Ca <sup>2+</sup>	0.0005	0.0001	0.0059
Sr <sup>2+</sup>	0.0061	0.0002	0.0052

TABLE III: Contributions to  $\alpha$  at different level of approximations in the many-body method.

Atoms	DF=MBPT(1)	MBPT(2)	MBPT(3)	CCSD
He	0.998	1.240	1.215	1.360
Li <sup>+</sup>	0.1579	0.1839	0.1851	0.1913
Be <sup>2+</sup>	0.0453	0.0510	0.0512	0.0521
Ne	1.977	2.254	1.654	2.652
Na <sup>+</sup>	0.8337	0.9154	0.8504	0.9984
Mg <sup>2+</sup>	0.4277	0.4555	0.4371	0.4852
Ar	10.152	9.964	8.005	11.089
K <sup>+</sup>	5.466	5.130	4.468	5.522
Ca <sup>2+</sup>	3.369	3.082	2.568	3.295
Kr	15.82	15.00	10.70	16.93
Rb <sup>+</sup>	9.273	8.374	7.103	9.213
Sr <sup>2+</sup>	6.146	5.388	4.492	5.877
Be	30.53	40.24	38.16	37.86
Mg	54.70	70.72	65.64	72.54
Ca	122.90	151.70	132.80	157.03
Sc <sup>+</sup>	50.10	57.17	47.02	53.24
Sr	156.83	188.98	163.13	186.98
Y <sup>+</sup>	68.60	75.42	65.10	72.26

tors have been used. Recently a similar approach, which had included the normalization of the wave function, had been used for evaluating the  $\alpha$ 's of some of the inert gas atoms [25, 26]. In fact, both these works account for non-linear terms at different level of approximations resulting in some differences in the results. Another calculation for the inert gas atoms was carried out by Nakajima and Hirao [43], where they have investigated the relativistic effects in  $\alpha$  using a scalar relativistic Douglas-Kroll (DK) Hamiltonian. The other difference between this work and

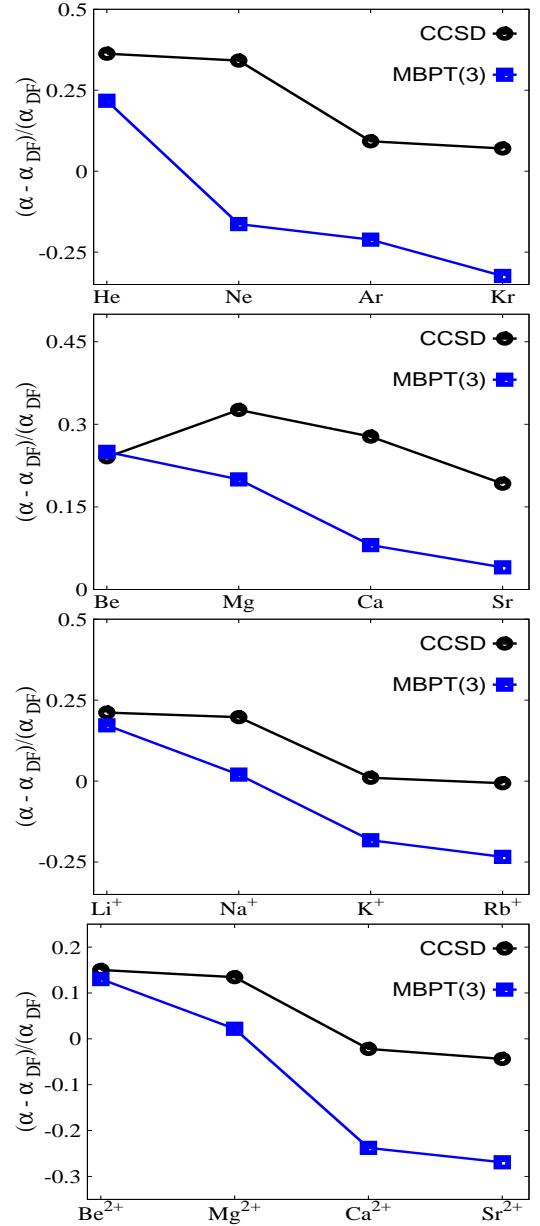


FIG. 11: (color online) Plots of  $(\alpha - \alpha_{DF})/\alpha_{DF}$  results versus atomic numbers from different groups of atomic systems.  $\alpha$  results are obtained using the MBPT(3) and CCSD methods in order to make a comparative study between these two approaches.

ours is that Nakajima and Hirao had estimated polarizability from the second order energy shift due to an arbitrary external electric field by a numerical finite field approach whereas we have evaluated this quantity by calculating the expectation value of the dipole operator using the first order dipole perturbed wave function. It is interesting that both the results agree fairly well with each other within the quoted uncertainties. For the alkaline earth elements we compare our results of  $\alpha$  with those of Porsev *et al.* [56, 71], who had used a hybrid approach combining the configuration interaction (CI) method in



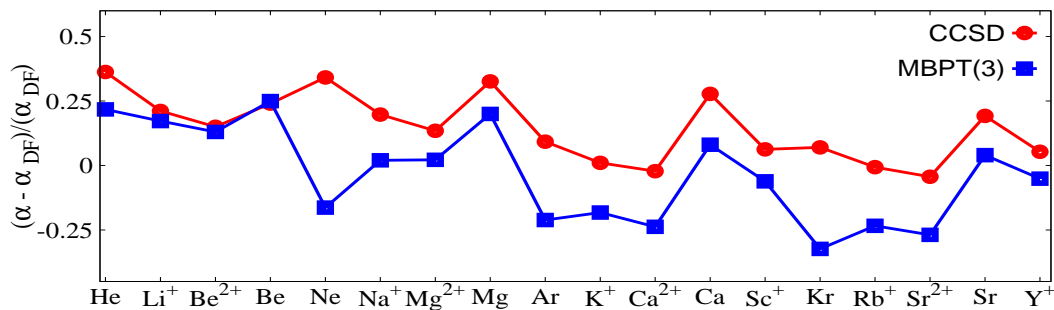


FIG. 12: (color online) Plots of MBPT(3) and CCSD  $(\alpha - \alpha_{DF})/\alpha_{DF}$  results for all the considered atoms and ions versus atomic numbers.

TABLE IV: Contributions from the RPA and non-RPA type of diagrams from the MBPT(3) method.

System	RPA	non-RPA
He	1.274	-0.059
Ne	2.303	-0.649
Ar	9.878	-1.873
Kr	14.980	-4.280
Be	36.788	1.372
Mg	65.074	0.566
Ca	135.459	-2.659
Sr	170.340	-7.210
Li <sup>+</sup>	0.1862	-0.0011
Na <sup>+</sup>	0.9261	-0.0757
K <sup>+</sup>	5.035	-0.567
Rb <sup>+</sup>	8.326	-1.223
Sc <sup>+</sup>	50.115	-3.095
Y <sup>+</sup>	67.181	-2.081
Be <sup>2+</sup>	0.0513	-0.0001
Mg <sup>2+</sup>	0.4627	-0.0256
Ca <sup>2+</sup>	3.009	-0.441
Sr <sup>2+</sup>	5.352	-0.860

the valence space and the MBPT method by scaling the energies and dressing the external electromagnetic field in the RPA framework to evaluate the core-polarization effects. Lim *et. al* [61] had performed the RCC calculations in the finite field method using the DK Hamiltonian. Our results for most of the atoms are in good agreement with them except for Sr which differs significantly. As mentioned in the previous section, we have found that higher order non-linear terms, especially those corresponding to RPA, are essential for obtaining accurate results. One probable reason for the discrepancies in the results between our RCC results and those of Porsev *et al.* is the treatment of core-core correlation effects in the two cases. We have computed these effects by the all order CCSD method, while they have used a finite order MBPT approach. An important difference between our approach and that of Lim *et. al* [61] is that we have used the proper DC Hamiltonian unlike its scalar components in [61] and the polarizabilities are estimated from the second order corrections to their calculated energies.

We now compare our results for the singly charged alkali-metal and doubly charged alkaline-earth-metal ions, which have electronic configurations similar to that of the inert gas atoms with the results obtained using the RPA method by Johnson *et. al.* [35] and another RCC calculation [27, 28]. The method employed in the latter calculations have already been referred to in the previous paragraph. The close agreement between the RPA and our RCC results is due to the fact that the dominant correlation effects in the evaluation of the polarizabilities for the closed-shell systems come from the core-polarization effects which are taken to all orders in both the calculations. We find from the MBPT(3) calculations that the non-RPA diagrams also contribute significantly in the closed-shell atoms. However, they cancel out to a large extent in these ions and their net contributions are consequently not significant. In another work, Lim *et. al* [72] have reported results for the alkali ions considering the scalar relativistic DK Hamiltonian and accounting for the spin-orbit coupling corrections through the MBPT(2) method using a fully relativistic four-component DF wave functions. In addition to the above mentioned systems we have also calculated  $\alpha$  for Sc<sup>+</sup> and Y<sup>+</sup> ions, but there are no data available for comparison with our results.

The main aim of the present work is to analyze the trends in the correlation effects in the static electric dipole polarizabilities of the ground states in a variety of closed shell atomic systems evaluated by different many-body methods in order to assess their potential for yielding accurate results for the coupling constants associated with the permanent electric dipole moments due to parity and time-reversal violations in atoms of experimental interest [73–79]. To fulfill our objective, we have carried out a range of calculations using lower order MBPT to MBPT(3) methods and have presented the results at each stage in Table III. These results are further compared with our final all order calculation using the relativistic CCSD method in the same table. This clearly demonstrates the importance of the correlation effects starting from lower to higher order perturbation theory systematically and provides a good understanding of their roles in obtaining accurate results. We have given results by grouping the iso-electronic systems together in this table in order to make a comparative analysis of the correlation

TABLE V: Contributions from various CCSD terms for the evaluation of  $\alpha$  in the ground states of the considered atomic systems.

System	$DT_1^{(1)}$	$T_1^{(0)\dagger}DT_1^{(1)}$	$T_2^{(0)\dagger}DT_1^{(1)}$	$T_2^{(0)\dagger}DT_2^{(1)}$	Others
He	1.362	0.005	-0.035	0.035	-0.007
Ne	2.613	0.073	-0.099	0.089	-0.024
Ar	11.806	-0.068	-1.143	0.511	-0.017
Kr	18.11	-1.12	-1.82	0.74	1.02
Be	39.45	-1.53	-7.21	3.84	3.31
Mg	75.66	-2.96	-10.16	5.54	4.46
Ca	163.87	-9.24	-24.89	16.05	11.24
Sr	201.90	-12.77	-28.77	15.57	11.05
Li <sup>+</sup>	0.1894	$\sim 0$	0.0019	0.0019	-0.0019
Na <sup>+</sup>	0.9756	$\sim 0$	-0.0005	$\sim 0$	0.0233
K <sup>+</sup>	5.972	-0.038	-0.620	0.211	-0.003
Rb <sup>+</sup>	9.971	-0.067	-1.049	0.333	0.025
Sc <sup>+</sup>	61.71	-2.16	-8.24	3.84	-1.91
Y <sup>+</sup>	83.19	-3.18	-10.68	5.05	-2.12
Be <sup>2+</sup>	0.0526	$\sim 0$	-0.0007	0.0003	-0.0001
Mg <sup>2+</sup>	0.4774	$\sim 0$	$\sim 0$	$\sim 0$	0.0078
Ca <sup>2+</sup>	3.578	-0.019	-0.585	0.117	0.204
Sr <sup>2+</sup>	6.396	-0.037	-0.689	0.191	0.016

effects as the atomic number varies. As can be seen in the table, the DF results are smaller than the MBPT results for the light inert gas atoms while this trend changes for the heavier ones. Finally, the CCSD results are larger than the DF results for all these atoms. Therefore this implies that there are strong cancellations between the correlation effects in these atoms and the higher order correlation effects play a pivotal role in determining the final results. A similar trend is also followed by other inert gas like singly charged alkali and doubly charged alkaline earth-metal ions. However, the trend for the correlation effects in the neutral alkaline earth-metal atoms is rather different. In this case the DF results are always smaller than those of MBPT and CCSD. In fact, it is also quite interesting to note that the correlation trends for Sc<sup>+</sup> and Y<sup>+</sup> do not follow those of other iso-electronic alkaline earth-metal atoms, but rather of the inert gas atoms. For a quantitative description, we plot  $(\alpha - \alpha_{DF})/\alpha_{DF}$  obtained using the MBPT(3) and CCSD methods versus atomic numbers in in Fig. 11 for the different categories of systems that we have considered. We also plot the same for all the systems together including Sc<sup>+</sup> and Y<sup>+</sup> ions in Fig. 12 to make a comparative analysis of the correlation trends among different iso-electronic sequences. To shed light on the role of different types of correlation effects that are crucial in the determination of polarizabilities and to explain the reasons for their trends in different iso-electronic sequences, we identify diagrams from the MBPT(3) approximation that belong to lower order RPA. We, then, present MBPT(3) results in Table IV classifying its diagrams as RPA and non-RPA types. As can be seen from Fig. 1 that all the diagrams up to MBPT(2) belong to RPA and hence, they are

the dominant contributors. However, diagrams shown in Fig. 1(vi-viii) are few examples of non-RPA type diagrams that also contribute significantly at the third order level, but they largely cancel out each other in the heavy atomic systems. The final results are the outcome of the interplay between these cancellations which can only be accounted correctly using an all order method like our CCSD method. This is evident from the contributions of the separate RCC terms presented below.

We now present the contributions from different correlation effects represented by the RCC terms in the evaluation of  $\alpha$  for different atomic systems. In Table V, we give the individual contribution from the important CCSD terms to  $\alpha$ , where the leading term  $DT_1^{(1)}$  contains the lowest order DF result. The next important term is  $T_2^{(0)\dagger}DT_1^{(1)}$  and the sign of its contribution is opposite to that of the former resulting in a substantial cancellation between these two largest contributors. In addition to the above two terms, contributions from  $T_1^{(0)\dagger}DT_1^{(1)}$  further reduce the final results. Pair excitations contributing through  $T_2^{(0)\dagger}DT_1^{(1)}$  and other higher order non-linear terms together take our final results towards the experimental values.

## V. CONCLUSION

We have employed the relativistic coupled-cluster method to calculate the static electric dipole polarizabilities of the ground states of many closed shell atomic systems. We have improved the results of our previous calculations for some of them by adding important non-linear RCC terms which correspond to higher order correlation effects in the present calculations. The crucial role of correlation effects is highlighted by presenting and comparing the results at different levels of approximations from lower order many-body perturbation theory to the relativistic CCSD method. Correlation trends among the neutral atoms, singly charged ions and doubly charged ions are presented. Investigation of various correlation effects in evaluating polarizabilities will provide valuable insights into the ongoing theoretical work on atomic electric dipole moments which arises due to parity and time-reversal symmetry violation. Our results will also serve as a guide to the future measurements of systems where the experimental values of polarizabilities are not precisely known.

## VI. ACKNOWLEDGMENT

We thank D. K. Nandy for his partial contribution in few parts of our programming. BKS and BPD were supported partly by INSA-JSPS under project no. IA/INSA-JSPS Project/2013-2016/February 28, 2013/4098. The computations reported in the present work were carried out using the 3TFLOP HPC cluster

at Physical Research Laboratory, Ahmedabad.

- 
- [1] C. J. Foot, *Atomic Physics*, Oxford University Press, Oxford, UK (2005).
  - [2] K. D. Bonin and V. V. Kresin, *Electric dipole polarizabilities of atoms, molecules and clusters*, World Scientific, Singapore (1997).
  - [3] C. J. Pethick and H. Smith, *Bose-Einstein Condensation in Dilute Gases*, Cambridge University Press, Cambridge, UK (2008).
  - [4] A. A. Madej and J. E. Bernard, *Frequency Measurement and Control*, edited by Andre N. Luiten, Topics in Applied Physics, v. 79, (Springer, Berlin, 2001), pp. 153195.
  - [5] W. D. Hall and J. C. Zorn, Phys. Rev. A **10**, 1141 (1974).
  - [6] R. W. Molof, H. L. Schwartz, T. M. Miller, and B. Bederson, Phys. Rev. A **10**, 1131 (1974).
  - [7] T. M. Miller and B. Bederson, Phys. Rev. A **14**, 1572 (1976).
  - [8] H. L. Schwartz, T. M. Miller, and B. Bederson, Phys. Rev. A **10**, 1924 (1974).
  - [9] A. D. Cronin, J. Schmiedmayer, and D. E. Pritchard, Rev. Mod. Phys. **81**, 1051 (2009).
  - [10] C. R. Ekstrom, J. Schmiedmayer, M. S. Chapman, T. D. Hammond, and D. E. Pritchard, Phys. Rev. A **51**, 3883 (1995).
  - [11] J. M. Amini and H. Gould, Phys. Rev. Lett. **91**, 153001 (Oct 2003).
  - [12] A. Dalgarno, Adv. Phys. **11**, 281 (1962).
  - [13] A. Dalgarno and H. A. J. McIntyre, Proc. Roy. Soc. **85**, 47 (1965).
  - [14] H. J. Monkhorst, Int. J. Quantum Chem. **12**(S11), 421 (1977).
  - [15] E. Dalgaard and H. J. Monkhorst, Phys. Rev. A **28**, 1217 (1983).
  - [16] B. Kundu and D. Mukherjee, Chem. Phys. Lett. **179**, 468 (1991).
  - [17] H. Koch, R. Kobayashi, A. Sanchez de Merás, and P. Jørgensen, J. Chem. Phys. **100**, 4393 (1994).
  - [18] R. Kobayashi, H. Koch and P. Jørgensen, J. Chem. Phys. **101**, 4956 (1994).
  - [19] B. Datta, P. Sen and D. Mukherjee, J. Phys. Chem. **99** (17), 64416451 (1995).
  - [20] K. Kowalski, J. R. Hammond and W. A. de Jong, J. Chem. Phys. **127**, 164105 (2007).
  - [21] J. R. Hammond, *Coupled-cluster Response Theory: Parallel Algorithms and Novel Applications*, PhD thesis submitted to Department of Chemistry, The University of Chicago, USA (2009).
  - [22] B. K. Sahoo and B. P. Das, Phys. Rev. A **77**, 062516 (2008).
  - [23] B. K. Sahoo, Chem. Phys. Lett. **448**, 144 (2007).
  - [24] B. K. Sahoo, B. P. Das, R. K. Chaudhuri and D. Mukherjee, J. Comp. Methods in Sci. and Engg. **7**, 57 (2007).
  - [25] S. Chattopadhyay, B. K. Mani and D. Angom, Phys. Rev. A **86**, 022522 (2012).
  - [26] S. Chattopadhyay, B. K. Mani and D. Angom, Phys. Rev. A **86**, 062508 (2012).
  - [27] S. Chattopadhyay, B. K. Mani and D. Angom, Phys. Rev. A **87**, 042520 (2013).
  - [28] S. Chattopadhyay, B. K. Mani and D. Angom, Phys. Rev. A **87**, 062504 (2013).
  - [29] I. Lindgren and J. Morrison, *Atomic Many-Body Theory*, Second Edition, Springer-Verlag, Berlin, Germany (1986).
  - [30] B. K. Sahoo, P. Mandal and M. Mukherjee, Phys. Rev. A **83**, 030502(R) (2011).
  - [31] J. Čížek, Adv. Chem. Phys. **14**, 35 (1969).
  - [32] V. Kvasnička, Phys. Rev. A **25**, 671 (1982).
  - [33] R. J. Bartlett and M. Musial, Rev. Mod. Phys. **79**, 291 (2007).
  - [34] F. E. Harris, Int. J. Quantum Chem. **75**, 593 (1999).
  - [35] W. R. Johnson, D. Kolb and K. Huang, At. Data Nucl. Data Table **28**, 333 (1983).
  - [36] P. Soldan, E. P. F. Lee and T. G. Wright, Phys. Chem. Chem. Phys. (Incorporating Faraday Transactions) **3**, 4661 (2001).
  - [37] D. Guban, and G. W. Michel, Molec. Phys. **39**, 783 (1980).
  - [38] D. Guban, and G. W. Michel, Metrologia **16**, 149 (1980).
  - [39] P. W. Langhoff, and M. Karplus, J. Opt. Soc. Am. **59**, 863 (1969).
  - [40] G. Lach, B. Jeziorski, and K. Szalewicz, Phys. Rev. Lett. **92**, 233001 (2004).
  - [41] A. Dalgarno, and A. E. Kingston, Proc. R. Soc. London A **259**, 424 (1960).
  - [42] J. W. Schmidt, R. M. Gaviolo, E. F. May, and M. R. Moldover, Phys. Rev. Lett. **98**, 254504 (2007).
  - [43] T. Nakajima, and K. Hirao, Chemistry Lett. **30**, 766 (2001).
  - [44] R. H. Orcutt, and R. H. Cole, J. Chem. Phys. **46**, 697 (1967).
  - [45] C. Gaiser, and B. Fellmuth, Europhys. Lett. **90**, 63002 (2010).
  - [46] K. Hald, F. Pawowski, P. Jrgensen, and C. Httig, J. Chem. Phys. **118**, 12921300 (2003).
  - [47] R. Franke, H. Mller, and J. Noga, J. Chem. Phys. **114**, 7746 (2001).
  - [48] C. Lupinetti and A. J. Thakkar, J. Chem. Phys. **122**, 044301 (2005).
  - [49] A. C. Newell, and R. C. Baird, J. Appl. Phys. **36**, 3751 (1965).
  - [50] A. J. Thakkar, H. Hetttema, and P. E. S. Wormer, J. Chem. Phys. **97**, 3252 (1992).
  - [51] J. Komasa, Phys. Rev. A **65**, 012506 (2001).
  - [52] D. Tunega, Chem. Phys. Lett. **269**, 435 (1997).
  - [53] G. L. Bendazzoli, and A. Monari, Chem. Phys. **306**, 153 (2004).
  - [54] W. Mller, J. Flesch, and W. Meyer, J. Chem. Phys. **80**, 3297 (1984).
  - [55] J. Mitroy, and M. W. J. Bromley, Phys. Rev. A **68**, 052714 (2003).
  - [56] S. G. Porsev and A. Derevianko, J. Exp. Theoret. Phys. (JETP) **102**, 195 (2006).
  - [57] E. F. Archibong, and A. J. Thakkar, Phys. Rev. A **44**, 5478 (1991).
  - [58] L. Hamonou, and A. Hibbert, J. Phys. B **41**, 245004 (2008).
  - [59] N. Reshetnikov, L. J. Curtis, M. S. Brown, and R. E.

- Irving, Phys. Scr. **77**, 015301 (2008).
- [60] R. Glass, J. Phys. B **20**, 4649 (1987).
  - [61] I. S. Lim and P. Schwerdtfeger, Phys. Rev. A **70**, 062501 (2004).
  - [62] A. J. Sadlej, M. Urban, and O. Gropen, Phys. Rev. A **44**, 5547 (1991).
  - [63] A. K. Bhatia and R. J. Drachman, Can. J. Phys. **75**, 11 (1997).
  - [64] W. R. Johnson and K. T. Cheng, Phys. Rev. A **53**, 1375 (1996).
  - [65] W. E. Cooke, T. F. Gallagher, R. M. Hill, and S. A. Edelstein, Phys. Rev. A **16**, 1141 (1977).
  - [66] U. Öpik, Proc. Phys. Soc. London **92**, 566 (1967).
  - [67] R. R. Freeman and D. Kleppner, Phys. Rev. A **14**, 1614 (1976).
  - [68] L. G. Gray, X. Sun, and K. B. MacAdam, Phys. Rev. A **38**, 4985 (1988).
  - [69] I. Johansson, Ark. Fys. **20**, 135 (1960).
  - [70] K. Bockasten, Phys. Rev. **102**, 729 (1956).
  - [71] S. G. Porsev and A. Derevianko, Phys. Rev. A **74**, 020502(R) (2006).
  - [72] I. S. Lim, J. K. Laerdahl and P. Schwerdtfeger, J. Chem. Phys. **116**, 172 (2002).
  - [73] M. A. Rosenberry and T. E. Chupp, Phys. Rev. Lett. **86**, 22 (2001).
  - [74] M. V. Romalis, W. C. Griffith, J. P. Jacobs, and E. N. Fortson, Phys. Rev. Lett. **86**, 2505 (2001).
  - [75] J. R. Guest, N. D. Scielzo, I. Ahmad, K. Bailey, J. P. Greene, R. J. Holt, Z.-T. Lu, T. P. OConnor, and D. H. Potterveld, Phys. Rev. Lett. **98**, 093001 (2007).
  - [76] W. C. Griffith, M. D. Swallows, T. H. Loftus, M. V. Romalis, B. R. Heckel, and E. N. Fortson, Phys. Rev. Lett. **102**, 101601 (2009).
  - [77] T. Furukawa, T. Inoue, T. Nanao, A. Yoshimi, M. Tsuchiya, H. Hayashi, M. Uchida, and K. Asahi, J. Phys. Conf. Ser. **312**, 102005 (2011).
  - [78] E. T. Rand, J. C. Bangay, L. Bianco, R. Dunlop, P. Finlay, P. E. Garrett, K. G. Leach, A. A. Phillips, C. S. Sumithrarachchi, C. E. Svensson, and J. Wong, J. Phys. Conf. Ser. **312**, 102013 (2011).
  - [79] T. Inoue, T. Furukawa, A. Yoshimi, Y. Ichikawa, M. Chikamori, Y. Ohtomo, M. Tsuchiya, N. Yoshida, H. Shirai, M. Uchida, K. Suzuki, T. Nanao, H. Miyatake, H. Ueno, Y. Matsuo, T. Fukuyama, and K. Asahi, Hyperfine Interactions **220**, 59 (Springer Netherlands, 2013).